Agglomerate TiO_2 Aerosol Dynamics at High Concentrations

Martin C. Heine, Sotiris E. Pratsinis*

(Received: 8 September 2006; accepted: 12 March 2007)

DOI: 10.1002/ppsc.200601076

In memoriam of Professor Dr. Brian Scarlett

Abstract

Primary and agglomerate particle dynamics are investigated for aerosol synthesis of titania at high solids concentrations that are typically used for its industrial scale manufacture. Particle formation and growth are simulated accounting for chemical reaction, coagulation and sintering. Process conditions are chosen so that the resulting primary and hard-agglomerate sizes are comparable with commercial product specifications. Neglecting aerosol polydispersity, the evolution of the diameter of primary particles, hard- and soft-agglomerates along with the agglomerate effective volume fraction are investigated. During synthesis of nanostructured titania (e.g. for catalysts and cosmetics) the effective soft-agglomerate volume fraction can exceed 30% within 100 s residence time indicating that a transition takes place from dilute to concentrated aerosol dynamics. At these conditions, classic Smoluchowski theory may no longer describe agglomerate coagulation and particles may affect fluid flow and heat transfer in industrial aerosol reactors. Furthermore, this could lead to restructuring and fragmentation of the product powder.

Keywords: aerosol dynamics, coagulation and sintering, fumed titania, hard- and soft-agglomerates

1 Introduction

Titanium dioxide is one of the most important ceramic materials. In 2000 about 4 million tons of titania pigment were produced world wide, about 60 % of those in aerosol reactors by combustion of $TiCl_4$ [1]. Typically its applications are in paints, papers, plastics, inks and even food or toothpaste. High surface area titania with primary particle size below 50 nm is transparent and so it is used in cosmetics and sunscreens as a thickener and for ultraviolet (UV) light absorption. Additionally it is an effective photocatalyst under UV light that is used to degrade organics in wastewater and industrial effluents.

Aerosol reactors are routinely used to manufacture nanoscale commodities resulting in products of high purity. In these reactors product primary and agglomerate particle sizes can be controlled by reactant concentration and particle residence time at high temperatures [2]. Their scale-up has been studied systematically by variation of precursor, oxidant and fuel flow rates [3]. Population balance models like monodisperse [4] and one- [5] or two-dimensional sectional [6] have been developed, revealing the details of particle growth accounting for chemical reaction, particle formation, coagulation and sintering.

For most applications the product specific surface area (SSA) and crystallinity are of key importance (e.g. pigments, catalysis), especially for nanosized powders. However, particle morphology, surface chemistry and degree of agglomeration can be equally important for final product performance [2]. Industrial aerosol reactors are usually operated at high precursor concentrations, close to stoichiometry, to achieve high reactor volume yields [1]. Then flame temperatures have to be

* M. C. Heine, S. E. Pratsinis, Particle Technology Laboratory, Institute of Process Engineering, Department of Mechanical and Process Engineering, ETH Zurich, 8092 Zürich (Switzerland).
E-mail: pratsinis@ptl.mavt.ethz.ch

controlled closely to quench primary particle growth once the desired SSA and crystallinity is reached.
Especially for nanosized materials such conditions result in large fractal-like or filamentary agglomerate structures where primary particles are only partially sintered (hard-agglomerates) and/or bond by weak physical forces (e.g. van der Waals forces) resulting in the so-called soft-agglomerates [7,8]. Those agglomerates can be much larger than constitutive primary particles and occupy far more space than a dense particle of equal mass. As a result, the effective particle volume fraction that includes entrapped gas increases with increasing number of primary particles per agglomerate of constant fractal dimension [9].
Here primary and agglomerate dynamics are investigated during formation and growth of TiO_2 particles by gas phase oxidation of $TiCl_4$ at high concentrations (close to stoichiometry: industrial precursor mole fraction near 50 % [10]). Such conditions are typical in manufacture of pigmentary titania with a primary particle size of 200–250 nm (SSA ~7 m^2/g) that is the second largest industrial aerosol-made product by value and volume (after carbon black) [3]. Results are compared also with nanostructured TiO_2 made by gas phase hydrolysis of $TiCl_4$ at high concentrations (initial precursor mole fraction about 10 %) [1]. Primary particle as well as hard- and soft-agglomerate diameters along with the degree of agglomeration are reported in the process parameter space of maximum reactor temperature and average cooling rate at fixed inlet $TiCl_4$ concentrations. Process conditions for synthesis of such particles are found to lie outside the standard assumptions of classic Smoluchowski coagulation theory based on the resulting effective agglomerate volume fraction.

2 Theory

2.1 Particle Formation and Dynamics

Pigmentary titania is typically produced by combustion of a preheated $TiCl_4/O_2$ mixture with the overall reaction [2]:

$$TiCl_4 + O_2 \xrightarrow{k} TiO_2 + 2Cl_2. \quad (1)$$

The consumption rate of $TiCl_4$ precursor follows a first-order reaction scheme with respect to $TiCl_4$ concentration [11]:

$$\frac{dC_{TiCl_4}}{dt} = -kC_{TiCl_4} = -\frac{dC_{TiO_2}}{dt} \quad (2)$$

where the rate constant $k(T)$ is given by the Arrhenius pre-exponential factor K and activation energy ΔE:

$$k = K\exp\left(\frac{-\Delta E}{\Re T}\right) \text{ with } K = 8.26\times10^4 s^{-1} \text{ and } \Delta E = 88.8 kJ/mol. \quad (3)$$

Alternatively titania can be synthesized by hydrolysis of $TiCl_4$ in a hydrogen/oxygen flame where a preheated H_2/air mixture reacts by fast exothermic oxidation of H_2. The resulting water steam then reacts stepwise with $TiCl_4$ [12] resulting in the overall reaction:

$$TiCl_4 + 2H_2O \longrightarrow TiO_2 + 4HCl. \quad (4)$$

Titania particles are formed by either of the above reactions (Eq. 1, 4) followed by coagulation and sintering. Neglecting primary particle polydispersity and surface growth [13,14], the evolution of the total particle number concentration, N (#/m^3_{gas}) is given by the monodisperse population balance (PB) [4]:

$$\frac{dN}{dt} = N_A\frac{dC_{TiO_2}}{dt} - \frac{1}{2}\beta N^2 \quad (5)$$

where N_A is Avogadro's number and β $(m^3/s/\#)$ is the appropriate collision frequency function [4, 15]. The rates of change of the total particle surface area, A (m^2/m^3_{gas}), and volume concentrations, V (m^3/m^3_{gas}) are:

$$\frac{dA}{dt} = N_A\frac{dC_{TiO_2}}{dt}a_m - \frac{1}{\tau_s}(A - Na_s) \text{ and}$$

$$\frac{dV}{dt} = N_A\frac{dC_{TiO_2}}{dt}v_m \quad (6)$$

where a_s (m^2) is the surface area of a completely fused (spherical) particle of volume V/N, while a_m and v_m are the area and volume of a monomer (TiO_2 molecule), respectively.
Besides particle dynamics the particle number, surface area and volume concentrations are also influenced by changes in the gas volume. Those changes typically result from gradients in process temperature or pressure and changes in overall gas stoichiometry, e.g. by chemical reaction or gas entrainment. These effects lead to source terms in Eqs. (5) and (6) that have been avoided by formulating aerosol concentrations per gas mass instead of the standard gas volume [5]. Eqs. (5) and (6) then directly account for changes in gas density and are valid for dilute and enclosed systems. During non-isothermal particle formation by chemical reaction at high

precursor concentrations, however, neither gas volume nor mass are preserved. For $TiCl_4$ oxidation (Eq. 1) and hydrolysis (Eq. 4) at stoichiometric conditions, the solid TiO_2 mass yield is 35 wt % of the initial gas mixture so even for $TiCl_4$ concentrations below the stoichiometric amount the gas mass during reaction is not constant. Additional source terms in Eqs. (5) and (6) can be avoided by balancing the total number flow of particles defined as product of N and gas volume flow Q, $\dot{N} = NQ$ (#/s) [16]. The $\dot{N}$ is independent of gas density and mass and only changes by particle dynamics. Similarly the rate of change for C in Eq. (2) can be replaced by $\dot{C} = CQ$ to be valid for the applied conditions. Eq. (5) is then given by:

$$\frac{d\dot{N}}{dt} = N_A \frac{d\dot{C}_{TiO_2}}{dt} - \frac{1}{2Q}\beta\dot{N}^2. \tag{7}$$

Here gas phase properties such as average molecular weight, density and viscosity that influence β are determined from all gaseous species including $TiCl_4$ but excluding TiO_2 particles (see Appendix). The population balances for particle surface area flow, $\dot{A} = AQ$ (m^2/s), and volume flow, $\dot{V} = VQ$ (m^3/s) can be obtained by replacing the concentrations A, C, N and V in Eq. (6) with the corresponding flows ($\dot{A}, \dot{C}, \dot{N}$ and $\dot{V}$) as described in the Appendix.

The effect of agglomerate structure in β is incorporated by the collision diameter d_c [4]:

$$d_c = d_p n_p^{1/Df} \tag{8}$$

where n_p is the average number of primaries per agglomerate and D_f is the mass fractal dimension of 1.8 as commonly used for aerosol-made agglomerates [17]. It should be noted here that for high soot agglomerate concentrations (near gelation) a $D_f = 2.6$ has been reported [18,19]. The characteristic time for sintering of titania is (SI units) [20]:

$$\tau_s = 7.4 \times 10^{16} T d_p^4 \exp\left(\frac{3.1 \times 10^4}{T}\right). \tag{9}$$

Particles are distinguished as non-, hard-, or soft-agglomerates [7]. Non-agglomerates are defined as fully-coalesced, dense particles where the primary and agglomerate particle diameter are identical ($d_c = d_p$). In flames these are typically formed at high temperatures followed by rapid cooling where particles fully coalesce upon collision [2]. Agglomerates that are held together by strong sintering necks, the so-called hard-agglomerates (aggregates), are formed at intermediate temperatures where characteristic times of coagulation, τ_{coag}, and sintering, τ_s (Eq. 9), are comparable [21]. Soft agglomerates are formed once sintering stops and d_p is constant [7]. These consist of either non- or hard-agglomerated particles that are held together only by weak physical forces. The transition from non- to hard-agglomerated particles is defined when d_c is 1 % larger than d_p. The transition from hard- to soft-agglomerates is defined when d_p becomes within 1 % of its final value, d_{pF}, and the corresponding d_c is the hard-agglomerate collision diameter, d_{cH} [7].

The effective agglomerate volume fraction, ϕ_c, is calculated from the agglomerate collision diameter by accounting for the entrapped gas [22]:

$$\phi_c = \frac{\pi}{6} N d_c^3. \tag{10}$$

For fully coalesced particles ϕ_c is identical with the solid volume fraction, ϕ_s, while ϕ_c increases for increasing degree of agglomeration.

2.2 Process Conditions and Numerical Integration

Industrial production of pigmentary titania by $TiCl_4$ oxidation proceeds at high temperature and production rates [1]. The $TiCl_4/O_2$ mixture preheated at $T_0 = 2000$ K is injected into the reactor that is operated at atmospheric pressure [10]. The inlet $TiCl_4$ fraction is 40 mol % resulting in full precursor conversion at high production rates [1]. The reactor temperature profile is adopted from Xiong and Pratsinis [10] resulting in a linear temperature increase from T_0 to T_{max} = 2500 K within 0.01 s and a subsequent linear temperature decrease by a cooling rate of CR = 2700 K/s corresponding to an external cooling flux of about 225 kJ/m^2/s.

Process conditions for synthesis of nanostructured titania by $TiCl_4$ hydrolysis are comparable to those of fumed silica production [1]. Here at atmospheric reactor pressure, the highest possible precursor ($TiCl_4$) concentrations are employed for 5 and 10 vol % of excess hydrogen and oxygen, respectively. Hence, the resulting initial gas composition of $TiCl_4/H_2/O_2/N_2$ = 1.0/2.1/1.1/4.3 [23] corresponds to a precursor $TiCl_4$ fraction of 11.8 mol %. Here, for simplicity, the H_2/O_2 combustion is not simulated and the initial stoichiometry is adapted assuming complete conversion of H_2 and O_2 to H_2O. This leads to a modified initial molar ratio of $TiCl_4/H_2O/O_2/N_2$ = 1.0/2.1/0.05/4.3.

3 Results and Discussion

3.1 Pigmentary TiO_2 Particle Dynamics made by $TiCl_4$ Oxidation

Figure 1 shows the evolution of process temperature, T (solid line), and $TiCl_4$ precursor conversion, X_{TiCl_4} (broken line), along with the TiO_2 solid particle volume fraction, ϕ_s (dash-dotted line). The gas inlet temperature of $T_0 = 2000$ K [10] increases by the exothermic oxidation reaction (Eq. 1) to reach $T_{max} = 2500$ K and complete precursor conversion ($X_{TiCl_4} > 99.9\,\%$) at $t = 0.01$ s. Cooling of the reactor walls and losses by heat radiation then decrease reactor temperature ($CR = 2700$ K/s) that drops below 1000 K at $t = 0.56$ s. During $TiCl_4$ conversion ($t < 0.01$ s) continuous TiO_2 formation increases the solid particle volume fraction to $\phi_s = 3.8 \times 10^{-3}\,\%$ at $t = 0.01$ s corresponding to $\phi_s = 3.2 \times 10^{-2}\,\%$ at room temperature. From this point on ϕ_s slightly increases from its dependence on gas density that steadily increases in the reactor cooling section ($t > 0.01$ s) until the gas temperature drops to that used for particle collection (e.g. at baghouse filter housing). Here this is set to 300 K [24].

In Figure 2 the corresponding evolution of the primary, d_p (solid line), and agglomerate, d_c (broken line), particle diameter is shown together with the effective agglomerate volume fraction, ϕ_c (Eq. 10; dash-dotted line). Once particle formation sets in, at about 2×10^{-6} s, molecular clusters grow initially by fully coalescing upon collision. As a result d_p and d_c are identical up to 0.013 s ($d_{pN} = 28.4$ nm, triangle) so particles are non-agglomerated. As particles grow further and temperature drops (Figure 1), their sintering rate slows down so particles coalesce only partially. As a result, hard-agglomerates form, until sintering effectively stops at $t = 0.22$ s when primary particles reach their final size of 200 nm. The corresponding hard-agglomerates consist of about 5 primary particles resulting in a collision diameter (open, circle) of $d_{cH} = 490$ nm [7]. Beyond this time particle collisions and coagulation continues, however, without any sintering, forming soft-agglomerates that are held together by physical rather than chemical forces.

The effective volume fraction ϕ_c in the pure coalescence period ($t \le 0.013$ s), where no agglomerates are formed, is equal to the solid volume fraction, ϕ_s, that is below $3.2 \times 10^{-2}\,\%$ at all times (Figure 1). However ϕ_c increases when agglomerates are formed ($t > 0.013$ s) as they occupy far more volume than their equivalent solid sphere mass [22,25]. At the onset of soft-agglomerate formation ϕ_c is about 0.015 % and steadily increases with residence time. Until $t = 10$ s ϕ_c is below 1 % so the effect of agglomerate volume fraction on the overall process might be minor. For $t > 10$ s however, soft-agglomerates occupy a significant amount of gas volume so particle dynamics will influence the overall transport phenomena (fluid flow, heat transfer) and vice versa. It should be noted that after complete reaction ($t = 0.01$ s) TiO_2 particles represent 33.6 wt % of the initial gas mass (2:1 gas to solid mass ratio) so they can affect overall gas properties even though ϕ_c is still negligible. Once the effective particle volume fraction becomes significant, the effect of particle volume fraction on the gas properties can be far more dramatic. Additionally the classic Smoluchowski equation for particle coagulation that was derived for infinitely dilute particle fractions will underpredict soft-agglomerate dynamics as a quasi-steady state concentration profile around the colliding particles cannot be sustained. At these conditions, coagulation could lead to gelation-restructuring for batch

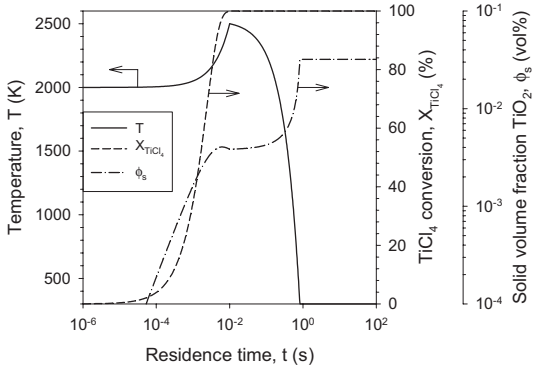

Fig. 1: Evolution of the flame temperature (solid line), $TiCl_4$ conversion by oxidation (broken line) and particle volume fraction (dash-dotted line) for synthesis of pigmentary titania for a maximum temperature of $T_{max} = 2500$ K ($T_0 = 2000$ K) and a cooling rate of $CR = 2700$ K/s similar to the process conditions of Xiong and Pratsinis (1991) [10].

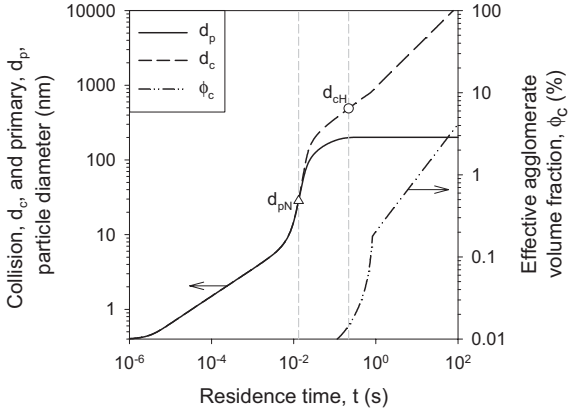

Fig. 2: Evolution of the primary (solid line) and agglomerate (broken line) particle size together with the effective agglomerate volume fraction (dash-double-dotted line) for $TiCl_4$ oxidation ($T_0 = 2000$ K, $T_{max} = 2500$ K, $CR = 2700$ K/s).

and flow systems [19,26]. Restructuring during coagulation will lead to larger D_f (e.g. 2.6 [19]) that will reduce ϕ_c and mitigate the effect of high concentration particle dynamics.

It should be noted that different process conditions can be applied to match the product properties of TiO_2 pigment. Elevated pressure and reduced T_{max} can also result in an average d_p of 200 nm. In general, increasing process pressure or precursor molarity results in higher ϕ_s and ϕ_c so the coupling between particle and transport phenomena becomes more significant and sets in at shorter reactor residence times.

3.2 Nanostructured TiO_2 Particle Dynamics made by $TiCl_4$ Hydrolysis

Nanostructured TiO_2 particles (d_p < 50 nm) can be tailor-made for specific applications by controlling the reactor temperature profile. This is typically achieved by adjusting inlet gas temperature and stoichiometry and by controlled cooling. Here the gas inlet temperature is T_0 = 1000 K and the initial $TiCl_4$ fraction is 11.8 mol % as for high SSA fumed silica manufacture [23]. The maximum reactor temperature, T_{max}, and cooling rate, CR, are the main parameters determining product specific surface area (SSA) and hard-agglomerate diameter, d_{cH}. Alternatively knowing the product properties (e.g. Degussa's P25 TiO_2) allows an estimation of T_{max} and CR.

Figures 3 and 4 show the evolution of d_p (solid line) and d_c (broken line) along with the effective agglomerate volume fraction, ϕ_c (dash-double-dot line, Eq. 10) and temperature profile (dash-dotted line) obtained by T_{max} = 1600 K and CR = 10,000 K/s. Resulting particles match the specifications of Aeroxide TiO_2 P25 (Degussa) with a Sauter mean diameter of about 30 nm (SSA = 50 m^2/g) and a hard-agglomerate (aggregate) diameter of 370 nm [27]. Detailed hydrolysis kinetics of $TiCl_4$ at high temperatures are not known so two limiting cases are shown for instantaneous and complete precursor conversion at $T = T_0$ (Figure 3) and $T = T_{max}$ (Figure 4).

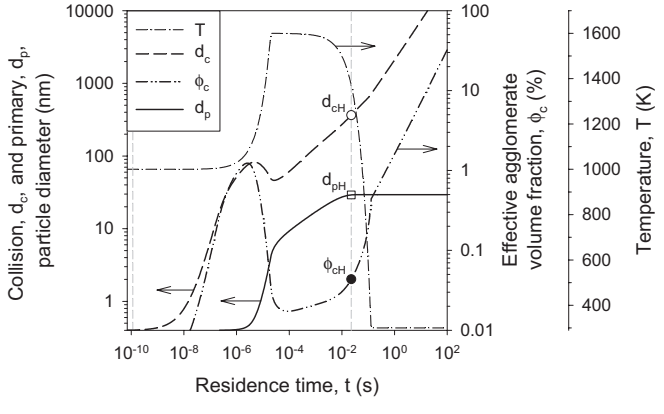

Fig. 3: Evolution of the primary (solid line) and agglomerate (broken line) particle diameter together with the effective agglomerate volume fraction (dash-double-dot line) and temperature profile (dash-dotted line) for T_0 = 1000 K, T_{max} = 1600 K, CR = 10,000 K/s and instantaneous and complete $TiCl_4$ hydrolysis at $T = T_{min}$. The product primary particle size (29 nm) and hard-agglomerate diameter (365 nm) are comparable to Aeroxide TiO_2 P25 specifications.

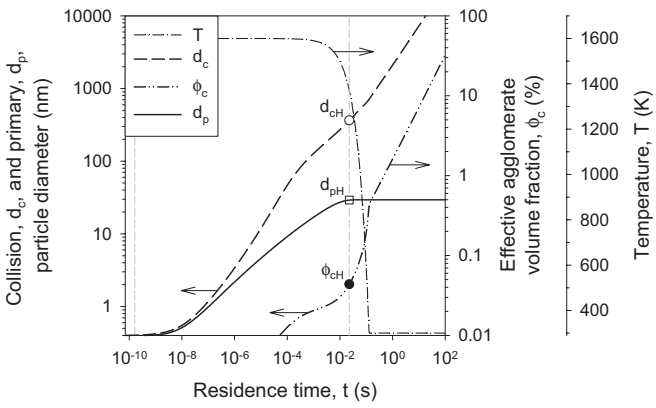

Fig. 4: Evolution of the primary (solid line) and agglomerate (broken line) particle size together with the effective agglomerate volume fraction (dash-double-dotted line) and temperature profile (dash-dotted line) for the process conditions of Figure 3 and instantaneous and complete $TiCl_4$ hydrolysis at $T = T_{max}$ (t = 0).

Initially (t < 0.001 s) particle dynamics are strongly influenced by chemical reaction and early particle formation. Complete $TiCl_4$ consumption at T_0 = 1000 K (Figure 3) leads to rapid agglomerate growth by coagulation while sintering is negligible until about 4.7×10^{-6} s (T = 1140 K) where characteristic times for coagulation, $\tau_{coag} = 2\,(\beta N)^{-1}$ [7], and sintering (Eq. 9) balance ($\tau_c \sim \tau_s = 6.4 \times 10^{-6}$ s) [28]. Up to this point, prior to the maximum process temperature, transient agglomerates are formed that are essentially molecular clusters [8]. At $t = 4.7 \times 10^{-6}$ s the d_c peaks with 82 nm and then drops to 46 nm at $t = 2.6 \times 10^{-5}$ s while d_p grows rapidly to 6 nm. This accelerated sintering results from the increased temperatures that are highest at T_{max} = 1600 K at $t = 2 \times 10^{-5}$ s. Consistent with d_c, the ϕ_c, also shows a peak (1.2 %) at 2.5×10^{-6} s that rapidly drops to 0.02 % at 9×10^{-5} s upon partial coalescence of these early agglomerates. As temperature drops after 0.02 s the ϕ_c steadily increases again to 32 % at 100 s.

In contrast to Figure 3, the initial temperature (t = 0) is highest ($T_0 = T_{max}$) in Figure 4 so d_p and d_c grow continuously by coagulation and sintering. Here no early peaks ($t < 10^{-4}$ s) of d_c and ϕ_c are observed. For t > 0.001 s, differences between Figure 3 and 4 vanish as particle properties are now determined by particle dynamics and residence time in the reactor cooling section. Sintering effectively stops at t = 0.023 s when primary

particles reach their final size of 29 nm (SSA = 53 m^2/g) for both cases. The corresponding hard-agglomerate collision diameter (open circle) and effective hard-agglomerate volume fraction (filled circle) are d_{cH} = 365 nm and ϕ_{cH} = 0.044 %, respectively, also for both cases. Differences in d_p, d_{cH} and ϕ_{cH} between Figure 3 and 4 are below 0.1 % showing that final agglomerate properties are not affected by the details of $TiCl_4$ hydrolysis as long as full $TiCl_4$ conversion is achieved. For $t > 0.023$ s particle collisions and coagulation continues, however, without any sintering. As a result, beyond this time, soft-agglomerates are formed.

Initially the effective volume fraction ϕ_c (dash-double-dotted line) equals the solid volume fraction ϕ_s that is between 1.8×10^{-3} and 9.6×10^{-3} % at T = 1600 and 300 K, respectively, and corresponds to 22.9 wt % of the initial gas mixture. Particle mass might influence gas properties but ϕ_s is too low for the particles to affect coagulation dynamics and overall transport phenomena. However ϕ_c increases when agglomerates are formed ($t > 10^{-9}$ s for Figure 3 and $t > 10^{-5}$ s for Figure 4) as they occupy far more volume than their equivalent solid sphere mass [22,25].

In fact during the onset of soft-agglomerate formation (t = 0.023 s), ϕ_c is already 0.044 % (filled circle) corresponding to the effective volume fraction of hard-agglomerates and steadily increases with residence time. Within t = 1 s, the ϕ_c reaches 1.6 % and even increases to 32 % at t = 100 s if agglomerates coagulate without restructuring or fragmentation for both cases. This indicates that for the industrially relevant high particle fractions and high specific surface areas, the effective volume fraction, ϕ_c, of particles can become significant. This might not affect the high temperature region in the reactor where d_p, SSA and d_{cH} are determined but it will most certainly affect their soft-agglomerate characteristics.

3.3 Hard-agglomerate Process Conditions

The above results show that ϕ_c can become important during synthesis of pigmentary titania by $TiCl_4$ oxidation (Figure 2) and even more during manufacture of nanostructured titania by $TiCl_4$ hydrolysis (Figures 3 and 4). As a result, the effect of reactor temperature (T_{max} and CR) on particle dynamics and especially on the effective volume fraction of hard- and soft-agglomerates is investigated here at industrially relevant high solid volume fractions.

Figure 5 shows the degree of hard-agglomeration, $h = d_{cH}/d_p$, as a function of T_{max} and CR for $TiCl_4$ hydrolysis at an initial $TiCl_4$ fraction of ϕ_0 = 11.8 mol % and complete $TiCl_4$ consumption at T_0 corresponding to Figure 4.

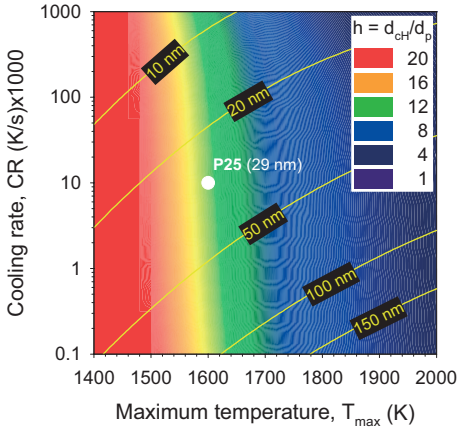

Fig. 5: Degree of agglomeration ($h = d_{cH}/d_p$) for titania produced by $TiCl_4$ hydrolysis in the process parameter space of cooling rate, CR, and maximum temperature, T_{max}, for an initial precursor mole fraction of ϕ_0 ($TiCl_4$) = 11.8 %. Isopleths (yellow lines) map the final primary particle diameter. Specific conditions that result in particles comparable to Aeroxide TiO_2 P25 (T_{max} = 1600 K and CR = 8,000 K/s) are marked (white circle).

The average d_p is shown as yellow isopleths. It is shown that T_{max} affects h more than CR consistent with Grass et al. [8]. The h increases for decreasing T_{max} as smaller but more numerous primary particles are formed, leading to large agglomerates in the hard-agglomerate region (Figure 4). Low CR also slightly increases h by prolonging particle residence times at intermediate temperatures. This then leads to extended particle necking and to formation of large hard-agglomerates [8]. The white circle corresponding to P25, h = 12.4 and d_p = 29 nm, indicates one specific process condition where d_p and d_{cH} are comparable to commercial Aeroxide TiO_2 P25 specifications. Isopleths of d_p show, that different operation conditions can be chosen to form powders with selected d_p. For d_p = 20 nm and ϕ_0 = 11.8, these are bound between $CR = 3000 - 10^6$ K/s and T_{max} = 1400 – 2000 K, leading to highly (h = 31) and sparsely agglomerated (h = 2.8) powders, respectively. In general, powders with larger d_p are less agglomerated and the degree of agglomeration at constant d_p (following the yellow isopleths) can be reduced by increasing T_{max} and CR [8,21].

Figure 6 shows the effect of T_{max} and CR on the hard-agglomerate effective volume fraction, ϕ_{cH} (filled circle in Figure 4) for the conditions of Figure 5. At low T_{max} the ϕ_{cH} is largest as h is highest (Figure 5) but even for T_{max} = 1400 K and CR = 100 K/s ϕ_{cH} is below 0.2 %. As a result, for all process conditions the influence of hard-agglomerates on the overall particle dynamics and transport phenomena is rather minor [29] as hard-agglomerate formation is described well by sintering and classic Smoluchowski coagulation theory.

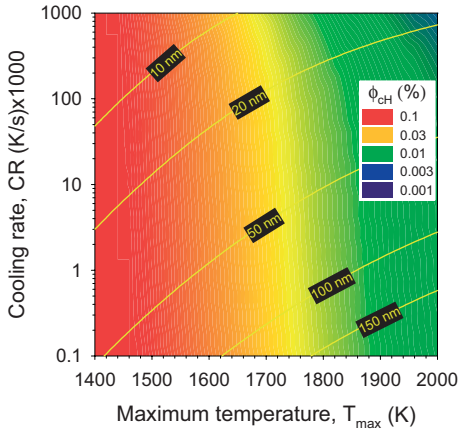

Fig. 6: Effective hard-agglomerate volume fraction, ϕ_{cH}, for titania particles in the process parameter space of cooling rate and maximum temperature. Isopleths show d_{pF} (yellow lines) for an initial precursor mole fraction of ϕ_0 ($TiCl_4$) = 11.8 %.

3.4 Soft-agglomerate Process Conditions

Contrary to ϕ_{cH}, the ϕ_{cS} depends on reactor residence time so a separate ϕ_{cS} agglomeration map is constructed for each such time. Figure 7 shows the evolution of the soft-agglomerate volume fraction, ϕ_{cS} (Eqs. 8, 10), at t = 0.1 a), b) 1, c) 10 and d) 100 s in the process parameter space of T_{max} and CR for the conditions of Figures 5 and 6. At t = 0.1 and 1 s, the d_p (yellow isopleths) still grows at T_{max} > 1800 K and CR < 10,000 K/s as

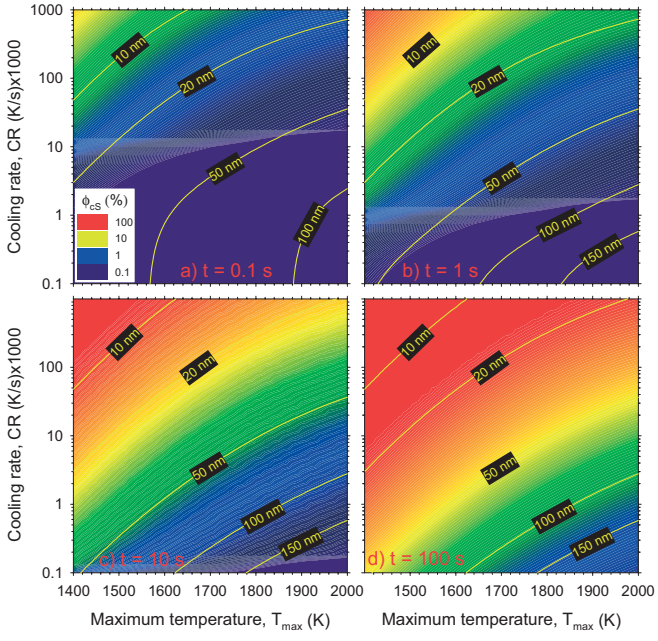

Fig. 7: Effective soft-agglomerate volume fraction, ϕ_{cS}, for titania particles at a) t = 0.1, b) 1, c) 10 and d) 100 s in the process parameter space of cooling rate and maximum temperature. Isopleths (yellow lines) show d_p at the corresponding residence time t.

reactor temperatures are still high enough for particle growth by sintering. For higher CR and lower T_{max}, however, the final d_p is already reached at t = 0.1 s. At t ≈ 1 s (Figure 7b), all primary particles with CR > 300 K/s reach their final size so sintering has ceased in most of the T_{max} – CR parameter space and agglomerates grow by coagulation only resulting in soft-agglomerates (non-blue regions).

Process conditions with low T_{max} and high CR result in the highest ϕ_{cS} as here d_p is smallest and the concentration of primary particles is highest. In contrast, large d_p form at high T_{max} and low CR so agglomerates are fewer and smaller resulting in low ϕ_{cS}. In general, isopleths for the effective soft-agglomerate volume fraction, ϕ_{cS}, are almost parallel to those of d_p. As time increases, the average agglomerate size grows by coagulation so according to Eqs. (8) and (10) ϕ_{cS} increases continuously from Figure 7a to 7d. Starting at t = 1 s all process conditions with CR > 7,000 K/s and T ≤ 1650 K result in effective volume fractions above 1 %, so agglomerate dynamics and transport phenomena might affect each other. For CR > 10,000 K/s and T_{max} < 1540 K ϕ_{cS} is even above 10 % at t = 10 s. For larger residence times the ϕ_{cS} can even become larger than unity (e.g. t = 100 s, CR > 30,000 K/s and T_{max} < 1500 K). This indicates that during TiO_2 formation at high concentrations the classic Smoluchowski theory for coagulation no longer holds for soft-agglomerate growth. As a result, at these conditions coagulation should proceed faster than predicted by classic theory and may include restructuring by forming denser agglomerates (larger D_f) as has been reported for soot [18,19]. Furthermore, it is possible that these soft-agglomerates may break and reform leading to narrower size distributions than the self-preserving limit [30].

4 Conclusions

Synthesis of TiO_2 by $TiCl_4$ oxidation was investigated at high concentrations (~40 mol % inlet $TiCl_4$) that are typically encountered in flame manufacture of pigmentary titania (d_p ~ 200 nm). Results are compared with flame hydrolysis of $TiCl_4$ that is commercially used for manufacture of nanostructured TiO_2 (~12 mol % $TiCl_4$). Accounting for coagulation and sintering and neglecting particle polydispersity, conditions for synthesis of hard- and soft-agglomerates were identified and related to the effective particle concentration in the reactor. In particular, for high specific surface area powders formed by $TiCl_4$ hydrolysis, a transition from dilute to concentrated particle dynamics was observed during soft-agglomerate formation within typical reactor residence times.

For $TiCl_4$ hydrolysis the influence of maximum reactor temperature and cooling rate on primary particle, hard-

and soft-agglomerate sizes and volume fractions was investigated. The effective volume fraction of the hard-agglomerates is below 0.2 % in the entire parameter space at the employed conditions indicating that specific surface area and hard-agglomerate diameter should be described well by classic coagulation theory and sintering. In contrast, the soft-agglomerate volume fraction quickly rises above 1 % or even 10 % for most process conditions. As a result, soft-agglomerate dynamics are not described by classic Smoluchowski coagulation theory. Furthermore soft-agglomerates should affect the overall gas flow, heat and mass transfer and restructuring or fragmentation of agglomerates.

5 Acknowledgements

Financial support by the Swiss National Science Foundation (SNF), 200020-107947/1, is gratefully acknowledged.

6 Nomenclature

a	particle surface area [m^2]
A	total particle surface area concentration [$m^2\ m^{-3}$]
$\dot{A}$	total particle surface area flow [$m^2\ s^{-1}$]
C	gas phase concentration [mol m^{-3}]
$\dot{C}$	molar flow [mol s^{-1}]
CR	cooling rate [K s^{-1}]
d	particle diameter [m]
D_f	fractal dimension [–]
ΔE	activation energy [J mol^{-1}]
h	degree of agglomeration [–]
i	index of chemical species [–]
k	reaction rate constant [s^{-1}]
K	Arrhenius pre–exponential factor [s^{-1}]
MW	molecular weight [kg mol^{-1}]
N	particle number concentration [m^{-3}]
$\dot{N}$	particle number flow [s^{-1}]
N_A	Avogadro's number [mol^{-1}]
Q	total gas flow [$m^3\ s^{-1}$]
$\Re$	ideal gas constant [J $mol^{-1}\ K^{-1}$]
t	time [s]
T	temperature [K]
v	particle volume [m^3]
V	total particle volume concentration [$m^3\ m^{-3}$]
$\dot{V}$	total particle volume flow [$m^3\ s^{-1}$]
X	precursor conversion [–]
y	gas mole fraction [–]

Greek Symbols

a_s	surface area of completely fused (spherical) particle [m^2]
β	particle collision frequency [$m^3\ s^{-1}$]
ϕ	volume fraction [–]
τ	characteristic time scale [s]

Indices

c	collision
$coag$	coagulation
F	final
H	hard
0	initial (t = 0)
m	monomer (molecule)
max	maximum
N	non-agglomerated (spherical)
p	primary
s	sintering
S	soft
s	solid

7 Appendix

Coagulation theory [31] describes the rate of change in particle volume concentration, N (#/m^3) as given by Eq. (5) for monodisperse particles. In contrast to liquid suspensions and isothermal, non-reactive aerosols, the fluid volume changes in flame aerosol reactors, e.g. by changes in gas temperature, pressure, stoichiometry or entrainment. The overall gas volume flow, Q (m^3/s), can change with particle residence time. In the absence of particle coagulation and fragmentation, however, the total number flow of particles, $\dot{N} = NQ$ (#/s), is constant. This directly results from the particle mass balance and is independent of Q. The change in N is then given as function of Q:

$$\frac{dN}{dt} = \frac{d(\dot{N}/Q)}{dt} = -\frac{\dot{N}}{Q^2}\frac{dQ}{dt} = -\frac{N}{Q}\frac{dQ}{dt}. \tag{11}$$

Combining Eq. (11) with changes in N by particle coagulation (Eq. (5), last term) results in:

$$\frac{dN}{dt} = -\frac{N}{Q}\frac{dQ}{dt} - \frac{1}{2}\beta N^2 \Longleftrightarrow \frac{1}{Q}\frac{d(NQ)}{dt} = -\frac{1}{2}\beta N^2. \tag{12}$$

This can be simplified further by expressing particle dynamics in respect of $\dot{N}$ instead of N:

$$\frac{d\dot{N}}{dt} = -\frac{1}{2Q}\beta\dot{N}^2. \tag{13}$$

Similarly, using $\dot{A} = AQ, \dot{V} = VQ$ and $\dot{C} = CQ$ instead of A, V and C, respectively, results in a modified particle surface area and volume balance:

$$\frac{d\dot{A}}{dt} = N_A \frac{d\dot{C}_{TiO_2}}{dt} a_m - \frac{1}{\tau_s}(\dot{A} - \dot{N}a_s) \text{ and}$$

$$\frac{d\dot{V}}{dt} = N_A \frac{d\dot{C}_{TiO_2}}{dt} v_m. \qquad (14)$$

The resulting set of Eqs. (7) and (14) is then independent of Q and can also be applied for conditions where high precursor concentrations lead to a significant reduction of gas mass during reaction.

Gas properties are obtained by averaging all gaseous species excluding solid TiO_2 particles. For example, the average molecular gas weight, $\overline{MW}$, is calculated by:

$$\overline{MW} = \sum_{i=1}^{i_{\max}} y_i MW_i \quad \text{with} \quad y_i = \dot{N}_i \Big/ \sum_{i=1}^{i_{\max}} \dot{N}_i \qquad (15)$$

where y_i is the gas mole fraction of species i = {$TiCl_4$, O_2, Cl_2} for $TiCl_4$ oxidation (i_{max} = 3) and {$TiCl_4$, O_2, H_2O, HCl, N_2} for $TiCl_4$ hydrolysis (i_{max} = 5).

8 References

[1] Ullmann, *Ullmann's Encyclopedia of Industrial Chemistry*, WILEY-VCH, **2005**.

[2] S. E. Pratsinis, Flame aerosol synthesis of ceramic powders. *Prog. Energy Combust. Sci.* **1998**, *24*, 197–219.

[3] K. Wegner, S. E. Pratsinis, Scale-up of nanoparticle synthesis in diffusion flame reactors. *Chem. Eng. Sci.* **2003**, *58*, 4581–4589.

[4] F. E. Kruis, K. A. Kusters, S. E. Pratsinis, B. Scarlett, A simple model for the evolution of the characteristics of aggregate particles undergoing coagulation and sintering. *Aerosol Sci. Technol.* **1993**, *19*, 514–526.

[5] S. Tsantilis, S. E. Pratsinis, Evolution of primary and aggregate particle-size distributions by coagulation and sintering. *AIChE J.* **2000**, *46*, 407–415.

[6] Y. Xiong, S. E. Pratsinis, Formation of agglomerate particles by coagulation and sintering. 1. A 2-dimensional solution of the population balance equation. *J. Aerosol Sci.* **1993**, *24*, 283–300.

[7] S. Tsantilis, S. E. Pratsinis, Soft- and hard-agglomerate aerosols made at high temperatures. *Langmuir* **2004**, *20*, 5933–5939.

[8] R. N. Grass, S. Tsantilis, S. E. Pratsinis, Design of high-temperature, gas-phase synthesis of hard or soft TiO_2 agglomerates. *AIChE J.* **2006**, *52*, 1318–1325.

[9] M. C. Heine, S. E. Pratsinis, High concentration agglomerate dynamics at high temperatures. *Langmuir* **2006**, *22*, 10238–10245.

[10] Y. Xiong, S. E. Pratsinis, Gas phase production of particles in reactive turbulent flows. *J. Aerosol Sci.* **1991**, *22*, 637–655.

[11] S. E. Pratsinis, H. Bai, P. Biswas, M. Frenklach, S. V. R. Mastrangelo, Kinetics of Titanium(IV) Chloride Oxidation. *J. Am. Ceram. Soc.* **1990**, *73*, 2158–2162.

[12] M. Rigo, P. Canu, L. Angelin, G. Della Valle, Kinetics of $TiCl_4$ hydrolysis in a moist atmosphere. *Ind. Eng. Chem. Res.* **1998**, *37*, 1189–1195.

[13] S. S. Talukdar, M. T. Swihart, Aerosol dynamics modeling of silicon nanoparticle formation during silane pyrolysis: a comparison of three solution methods. *J. Aerosol Sci.* **2004**, *35*, 889–908.

[14] S. Tsantilis, S. E. Pratsinis, Narrowing the size distribution of aerosol-made titania by surface growth and coagulation. *J. Aerosol Sci.* **2004**, *35*, 405–420.

[15] J. H. Seinfeld, *Atmospheric Chemistry and Physics of Air Pollution*. John Wiley and Sons, New York, **1986**.

[16] M. C. Heine, S. E. Pratsinis, Droplet and particle dynamics during flame spray synthesis of nanoparticles. *Ind. Eng. Chem. Res.* **2005**, *44*, 6222–6232.

[17] D. W. Schaefer, A. J. Hurd, Growth and structure of combustion aerosols – Fumed silica. *Aerosol Sci. Technol.* **1990**, *12*, 876–890.

[18] C. M. Sorensen, W. Kim, D. Fry, D. Shi, A. Chakrabarti, Observation of soot superaggregates with a fractal dimension of 2.6 in laminar acetylene/air diffusion flames. *Langmuir* **2003**, *19*, 7560–7563.

[19] W. Y. Kim, C. M. Sorensen, D. Fry, A. Chakrabarti, Soot aggregates, superaggregates and gel-like networks in laminar diffusion flames. *J. Aerosol. Sci.* **2006**, *37*, 386–401.

[20] A. Kobata, K. Kusakabe, S. Morooka, Growth and Transformation of TiO_2 Crystallites in Aerosol Reactor. *AIChE J.* **1991**, *37*, 347–359.

[21] R. S. Windeler, K. E. J. Lehtinen, S. K. Friedlander, Production of nanometer-sized metal oxide particles by gas phase reaction in a free jet. 2. Particle size and neck formation – Comparison with theory. *Aerosol Sci. Technol.* **1997**, *27*, 191–205.

[22] K. A. Kusters, J. G. Wijers, D. Thoenes, Aggregation kinetics of small particles in agitated vessels. *Chem. Eng. Sci.* **1997**, *52*, 107–121.

[23] B. Hannebauer, F. Menzel, The combustion of $SiCl_4$ in hot O_2/H_2 flames. *Z. Anorg. Allg. Chem.* **2003**, *629*, 1485–1490.

[24] S. Tsantilis, H. K. Kammler, S. E. Pratsinis, Population balance modeling of flame synthesis of titania nanoparticles. *Chem. Eng. Sci.* **2002**, *57*, 2139–2156.

[25] J. C. Flesch, P. T. Spicer, S. E. Pratsinis, Laminar and Turbulent Shear-Induced Flocculation of Fractal Aggregates. *AIChE J.* **1999**, *45*, 1114–1124.

[26] F. O. Ernst, S. E. Pratsinis, Self-preservation and gelation during turbulence-induced coagulation. *J. Aerosol Sci.* **2006**, *37*, 123–142.

[27] D. Gumy, C. Morais, P. Bowen, C. Pulgarin, S. Giraldo, R. Hajdu, J. Kiwi, Catalytic activity of commercial of TiO_2 powders for the abatement of the bacteria (E-coli) under solar simulated light: Influence of the isoelectric point. *Appl. Catal. B-Environ.* **2006**, *63*, 76–84.

[28] R. S. Windeler, S. K. Friedlander, K. E. J. Lehtinen, Production of nanometer-sized metal oxide particles by gas phase reaction in a free jet. 1. Experimental system and results. *Aerosol Sci. Technol.* **1997**, *27*, 174–190.

[29] D. Quemada, Rheological modelling of complex fluids. I. The concept of effective volume fraction revisited. *Eur. Phys. J.-Appl. Phys.* **1998**, *1*, 119–127.

[30] S. J. Harris, M. M. Maricq, The role of fragmentation in defining the signature size distribution of diesel soot. *J. Aerosol Sci.* **2002**, *33*, 935–942.

[31] M. Smoluchowski, Versuch einer mathematischen Theorie der Koagulationskinetik kolloider Lösungen. *Z. Physik. Chem.* **1917**, *92*, 129–168.

